

Science Foundation. We are most grateful to Dr. Gordon Rodley for synthesizing single crystals suitable for X-ray analysis.

**Supplementary Material Available.** A listing of structure factor amplitudes will appear following these pages in the microfilm edition of this volume of the journal. Photocopies of the supplementary

material from this paper only or microfiche (105 × 148 mm, 24× reduction, negatives) containing all of the supplementary material for the papers in this issue may be obtained from the Journals Department, American Chemical Society, 1155 16th St., N.W., Washington, D. C. 20036. Remit check or money order for \$3.00 for photocopy or \$2.00 for microfiche, referring to code number JACS-74-4428.

## Kinetics and Thermodynamics of Rapid Structural Interconversions of Dichloro-1,1,7,7-tetraethyldiethylenetriaminenickel(II) in Acetonitrile

Hideo Hirohara, Kenneth J. Ivin, John J. McGarvey,\* and John Wilson

Contribution from the Department of Chemistry, The Queen's University of Belfast, Belfast, BT9 5AG, Northern Ireland. Received January 3, 1974

**Abstract:** Spectrophotometric and conductometric studies in acetonitrile solutions of dichloro-1,1,7,7-tetraethyldiethylenetriaminenickel(II) ( $\text{NiLCl}_2$  where L is the tridentate ligand 1,1,7,7-tetraethyldiethylenetriamine) are interpreted in terms of the following equilibria, where  $\text{NiLCl}^+||\text{Cl}^-$  represents an outer-sphere complex:  $\text{NiLCl}_2 \rightleftharpoons \text{NiLCl}^+||\text{Cl}^- \rightleftharpoons \text{NiLCl}^+ + \text{Cl}^-$  (eq 2). The equilibrium constants have the following values at 20°:  $K_1 = k_{12}/k_{21} = 0.95$ ;  $K_s = k_{23}/k_{32} = 8 \times 10^{-5} \text{ mol dm}^{-3}$ ;  $K_d = K_1 K_s / (1 + K_1) = 3.9 \times 10^{-5} \text{ mol dm}^{-3}$ . Values of  $\Delta H^\circ$  and  $\Delta S^\circ$  were also determined. Kinetic data for this system were obtained by relaxation methods, in which the equilibria were suddenly perturbed by an electric field jump or by means of a pulse of radiation from a Q-switched neodymium laser. The results were interpreted in terms of the above mechanism; values for the rate constants  $k_{21}$  and  $k_{32}$  were estimated to be  $7 \times 10^5 \text{ sec}^{-1}$  and  $2 \times 10^9 \text{ M}^{-1} \text{ sec}^{-1}$ , respectively, at 20°.

Although five-coordination is somewhat unusual<sup>1</sup> for nickel(II) compounds, a considerable number of complexes of this type have now been prepared and characterized.<sup>2</sup> The complexes frequently contain bulky, polydentate ligands so that the tendency to attain six-coordination is suppressed by crowding around the central metal ion. As well as being of stereochemical interest, five-coordinate species have frequently been proposed as intermediates in substitution reactions<sup>3</sup> and structural interconversions<sup>4,5</sup> of transition metal complexes.

One example of a nickel(II) compound which can exist in a stable five-coordinate form is dichloro-1,1,7,7-tetraethyldiethylenetriaminenickel(II), written as  $\text{NiLCl}_2$ , where L is the tridentate ligand  $\text{Et}_2\text{N}(\text{CH}_2)_2\text{NH}(\text{CH}_2)_2\text{NEt}_2$ . On the basis of spectral, magnetic, and conductometric evidence, Dori and Gray<sup>6</sup> showed that in acetonitrile and other polar organic solvents this compound was capable of existing in at least two stereochemical modifications present in equilibrium: a five-coordinate, paramagnetic, un-ionized species  $\text{NiLCl}_2$  (absorption maximum 450 nm) and a four-coordinate, square-planar, diamagnetic, ionized species  $\text{NiLCl}^+$  (absorption maximum 530 nm). In describing

(1) P. Orioli, *Coord. Chem. Rev.*, **6**, 285 (1971).

(2) B. F. Hoskins and F. D. Williams, *Coord. Chem. Rev.*, **9**, 365 (1973).

(3) E.g., M. L. Tobe, "Inorganic Reaction Mechanisms," Nelson, London, 1972.

(4) R. D. Farina and J. H. Swinehart, *J. Amer. Chem. Soc.*, **91**, 568 (1969).

(5) K. J. Ivin, R. Jamison and J. J. McGarvey, *J. Amer. Chem. Soc.*, **94**, 1763 (1972).

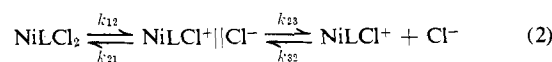
(6) Z. Dori and H. B. Gray, *J. Amer. Chem. Soc.*, **88**, 1394 (1966).



these species as five- and four-coordinate, respectively, one is ignoring the possibility of weak coordination by the solvent. This point is discussed later.

In the present paper we describe a kinetic and thermodynamic investigation of this system in acetonitrile as solvent. Two chemical relaxation methods were applied. In the first method the position of the equilibrium was disturbed by application of an electric field pulse (second Wien effect).<sup>7</sup> This method could be used because  $\text{NiLCl}_2$  behaves as a moderately weak electrolyte in acetonitrile. The second method depends on the fact that  $\text{NiLCl}_2$  absorbs at 1.06  $\mu\text{m}$ , and it was found possible to disturb the equilibrium by means of a pulse of radiation from a Q-switched neodymium laser operating at this wavelength. Conductometric and spectrophotometric methods were used to monitor the relaxation processes as well as to investigate the equilibrium itself.

Both the kinetic and thermodynamic results indicate the participation of a third species in the equilibrium. This is postulated to be an outer-sphere complex written as  $\text{NiLCl}^+||\text{Cl}^-$ . The equilibria are thus represented by (2) where  $k_{12}$ , etc., denote the rate constants.



### Experimental Section

**Kinetics.** The Q-switched neodymium laser and spectrophoto-

(7) M. Wien and J. Schiele, *Z. Phys.*, **32**, 545 (1931).

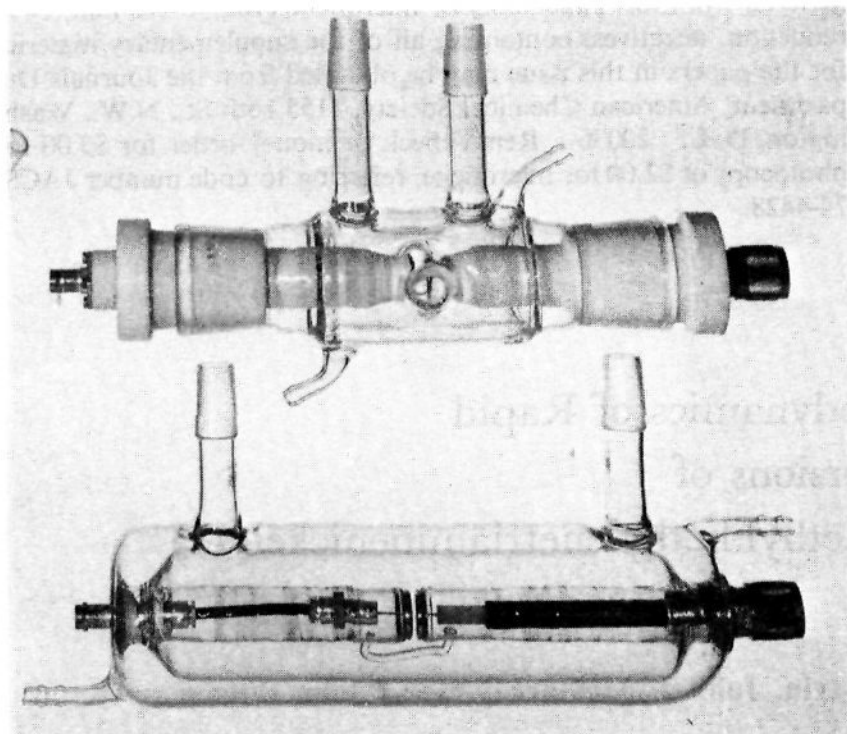


**Figure 1.** Conductivity cells used for DFE relaxation studies: bottom, sample cell; top, reference cell.

metric detection system have been described elsewhere.<sup>8</sup> The laser pulse had a half-width of about 70 nsec; pulse energies in the range 0.15–0.4 J were used. Absorbance changes in the solutions were recorded at 450 and 530 nm by means of a Solartron CD 1700 or a Hewlett-Packard 181A oscilloscope. The detection system had a minimum response time of 50 nsec and was capable of detecting absorbance changes of  $>0.4\%$  at the fastest oscilloscope sweep rates used ( $50 \text{ nsec cm}^{-1}$ ).

The electric field-jump apparatus was based on the designs of Eyring, *et al.*,<sup>9</sup> and of Staples, Turner, and Atkinson.<sup>10</sup> High voltage pulses were generated by means of the coaxial delay-line technique.<sup>11</sup> The coaxial cable (1000 m of Uniradio Type 67) was charged through a limiting resistance from a high voltage supply (Hursant Ltd. Model 30B) and discharged into a termination matched to the characteristic impedance ( $50 \Omega$ ) of the cable. The pulses had a rise time of less than  $0.2 \mu\text{sec}$ , a duration of  $9.2 \mu\text{sec}$ , and a fall time of about  $2 \mu\text{sec}$ .

Figure 1 shows the sample and reference cells. The electrodes, 2.5 cm diameter and 1 mm thick, were constructed from platinum. In the sample cell, they were fused into the ends of soft glass/Pyrex graded seals, the interelectrode distance being fixed at 2.5 mm. In the reference cell the interelectrode distance was variable (2–10 mm), and in this case the electrodes were pressed tightly (without an adhesive) into the ends of Teflon tubes. Before assembling the cells, the electrodes were polished to remove all scratches and sharp edges. Both cells were immersed in a bath of silicone oil, the temperature of which was held constant to better than  $0.1^\circ$ .

The rapid changes in conductance following perturbation of the weak electrolyte equilibrium were followed by means of the rapid changes in voltage across an asymmetric Wheatstone bridge. The sample and reference cells formed two arms of the bridge,  $(3.5\text{--}8.6) \times 10^3 \Omega$ , the other two arms being low resistance terminations,  $20\text{--}50 \Omega$ . The voltage changes across the bridge were recorded on a Hewlett-Packard 181A oscilloscope, fitted with a differential amplifier (type 1803A). The asymmetry of the bridge ensured that the output signals from the bridge to the differential amplifier remained below 50 V, thereby eliminating the need for high voltage attenuators at the oscilloscope inputs and making it easier to balance the bridge.<sup>9</sup> In order to compensate for the small increase in conductance in the sample cell resulting from the first Wien effect,<sup>12</sup> it was balanced against a reference cell containing a solution of a

strong electrolyte (approximately  $10^{-4} M \text{ NaBPh}_4$ ) in the same solvent.<sup>13</sup>

At the start of the experiment the interelectrode distance in the reference cell was set at 2.5 mm and the concentration of the strong electrolyte was adjusted until the conductance of the reference cell (measured with a 1000-Hz impedance bridge, Wayne Kerr Model B221A) matched that of the sample cell. Small adjustments were then made in the concentration of strong electrolyte and the interelectrode spacing until both conductance and capacitance matched as closely as possible. Considerable efforts were made to keep the capacitance mismatch as small as possible ( $<60 \text{ pF}$ ), since otherwise pronounced ringing effects and voltage spikes were subsequently observed at the leading edge of the high voltage pulse.

Following the above matching procedure at zero field, the Wheatstone bridge was balanced at a voltage of 2 kV ( $\equiv 8 \text{ kV cm}^{-1}$  for an interelectrode separation of 2.5 mm). At this voltage the dissociation field effect was just detectable, and slight adjustments were again made to the strong electrolyte concentration and/or the interelectrode separation in the reference cell until a horizontal trace was observed on the oscilloscope. Application of higher fields resulted in readily detectable dissociation field effects. The highest field strength attainable in the cells was  $30 \text{ kV cm}^{-1}$ , the limit being set partly by the breakdown voltage of the connectors (type UG212 C/U) to the high voltage cable and partly by the need to maintain adequate interelectrode separations in order to minimize surface effects.<sup>14</sup> Noise on the relaxation traces was reduced by screening the connections to the electrodes in both cells.

**Equilibria.** Ultraviolet, visible, and near-infrared spectra were recorded on Perkin-Elmer 402 and Cary 17 spectrophotometers. For the determination of equilibrium constants absorbances were measured on a Unicam SP500 spectrophotometer using thermostated 1-cm silica cells.

Conductivity measurements were made on a Wayne-Kerr bridge (Model B221A), with the temperature of the conductance cell controlled to  $\pm 0.02^\circ$ . The cell constant was  $0.246 \text{ cm}^{-1}$ . The data were treated according to the method of Fuoss<sup>15</sup> in order to obtain the limiting molar conductance  $\Lambda_0$  and the limiting (activity) dissociation constant  $(K_d)_0$  at zero ionic strength. In this method the required activity coefficients were calculated from the Debye-Hückel limiting equation; only the points at concentrations below  $2.5 \times 10^{-4} M$  were used for the final linear extrapolation performed by the method of least squares.

**Materials.**  $\text{NiCl}_2$  was prepared according to the method of Dori and Gray<sup>6</sup> and recrystallized from ethanol containing a small amount of acetone. Acetonitrile (Analar) was purified as described by Riddick and Bunger.<sup>16</sup>

## Results and Discussion

**Equilibria.** The values of  $\Lambda_0$  and  $(K_d)_0$  determined conductometrically are shown in Table I. The values of  $K_d$  determined spectrophotometrically on the basis of

**Table I.** Limiting Molar Conductances, Equilibrium Constants, and Thermodynamic Parameters for  $\text{NiCl}_2$  in Acetonitrile ( $L = 1,1,7,7\text{-tetraethyl-diethylenetriamine}$ )

Temp, $^\circ\text{C}$	$\Lambda_0, \text{cm}^2 \text{ mol}^{-1} \Omega^{-1}$	$10^5(K_d)_0, \text{mol dm}^{-3}$	$(K_1)_0$	$10^5(K_s)_0, \text{mol dm}^{-3}$
20	$229 \pm 10$	$3.93 \pm 0.10$	$0.95 \pm 0.01$	$8.05 \pm 0.20$
25	$242 \pm 7$	$3.75 \pm 0.07$	$0.90 \pm 0.02$	$7.91 \pm 0.14$
30	$253 \pm 7$	$3.50 \pm 0.11$	$0.85 \pm 0.02$	$7.65 \pm 0.22$
35	$280 \pm 10$	$3.23 \pm 0.10$	$0.80 \pm 0.02$	$7.28 \pm 0.25$
40	$306 \pm 15$	$2.96 \pm 0.18$	$0.76 \pm 0.01$	$6.86 \pm 0.35$
45	$329 \pm 16$	$2.70 \pm 0.14$	$0.72 \pm 0.02$	$6.47 \pm 0.37$
50	$353 \pm 18$	$2.40 \pm 0.12$	$0.68 \pm 0.01$	$5.96 \pm 0.30$
$\Delta H^\circ/\text{kJ mol}^{-1}$ (av for 20–50 $^\circ$ )			–9.2	–7.8
$\Delta S^\circ/\text{J K}^{-1} \text{ mol}^{-1}$ (av for 20–50 $^\circ$ )			–32.0	–105.0

(8) R. Jamison, Ph.D. Thesis, The Queen's University of Belfast, 1972.

(9) D. T. Rampton, L. P. Holmes, D. L. Cole, R. P. Jensen, and E. M. Eyring, *Rev. Sci. Instrum.*, **38**, 1637 (1967).

(10) B. R. Staples, D. J. Turner, and G. Atkinson, *Chem. Instrum.*, **2**, 127 (1969).

(11) M. Eigen and L. DeMaeyer in "Techniques of Organic Chemistry," Vol. 8, Part II, 2nd ed, S. L. Friess, E. S. Lewis, and A. Weissberger, Ed., Interscience, New York, N. Y., 1963, p 988 ff.

(12) M. Wien, *Ann. Phys. (Leipzig)*, **83**, 327 (1927).

(13) R. L. Kay, B. J. Hales, and G. P. Cunningham, *J. Phys. Chem.*, **71**, 3925 (1967).

(14) Reference 11, p 989.

(15) R. M. Fuoss, *J. Amer. Chem. Soc.*, **57**, 488 (1935); R. M. Fuoss and F. Accascina, "Electrolytic Conductance," Interscience, New York, N. Y., 1959.

(16) J. A. Riddick and W. P. Bunger in "Techniques of Chemistry," Vol. II, A. Weissberger, Ed., Wiley-Interscience, New York, N. Y., 1970, p 801.

eq 1, over the concentration range  $(2.5-10) \times 10^{-3} M$ , were 40-140 times larger than the values of  $(K_d)_0$  determined conductometrically and varied by a factor of four in this concentration range. These discrepancies are much too large to be accounted for in terms of variations in the activity coefficients. Furthermore the plot of  $\log (K_d)_0$  against  $T^{-1}$  is curved convex toward the  $\log (K_d)_0$  axis; see Figure 2, curve A. These facts lead us to postulate the two-stage (2) with equilibrium constants defined by (3) and (4). The ionic dissociation

$$K_i = k_{12}/k_{21} = [\text{NiLCl}^+||\text{Cl}^-]/[\text{NiLCl}_2] \quad (3)$$

$$K_s = k_{23}/k_{32} = [\text{NiLCl}^+][\text{Cl}^-]/[\text{NiLCl}^+||\text{Cl}^-] \quad (4)$$

tion constant  $K_d$ , defined by (5), is then related to  $K_i$

$$K_d = \frac{[\text{NiLCl}^+][\text{Cl}^-]}{[\text{NiLCl}_2] + [\text{NiLCl}^+||\text{Cl}^-]} \quad (5)$$

and  $K_s$  by (6).

$$K_d = K_i K_s / (1 + K_i) \quad (6)$$

In order to reinterpret the spectrophotometric evidence on this basis, it is necessary to assume that the outer-sphere complex  $\text{NiLCl}^+||\text{Cl}^-$  has the same absorption spectrum as the free ion  $\text{NiLCl}^+$ . This is a reasonable assumption<sup>17</sup> since the  $\text{Cl}^-$  ion is so far removed from the central nickel ion that it is unlikely to influence the splitting of the d energy levels or the transition probability. Further support for this assumption is provided by the work of Hogen-Esch and Smid<sup>18</sup> on alkali metal fluorenyls in tetrahydrofuran where no difference could be detected in the absorption maxima of solvent-separated ion pairs and free fluorenyl carbanions. In the present system it may also be noted that the band maximum of four-coordinate species in other solvents is not substantially shifted from that recorded in acetonitrile<sup>6</sup> indicating that any solvent coordination is very weak. The extinction coefficient  $\epsilon$  at 540 nm of  $\text{NiLCl}^+||\text{Cl}^-$  and  $\text{NiLCl}^+$  was determined in ethanol where the complex exists<sup>6</sup> only as the four-coordinate species. The value obtained for  $\epsilon$  was<sup>19</sup>  $180 M^{-1} \text{cm}^{-1}$ .

If the absorbance at 540 nm for a depth of 1 cm is  $A$ , we may write

$$A/\epsilon = [\text{NiLCl}^+||\text{Cl}^-] + [\text{NiLCl}^+] \quad (7)$$

also

$$\alpha C_0 = [\text{NiLCl}^+] \quad (8)$$

where

$$C_0 = [\text{NiLCl}^+] + [\text{NiLCl}^+||\text{Cl}^-] + [\text{NiLCl}_2] \quad (9)$$

and  $\alpha$  is the degree of dissociation calculated from  $(K_d)_0$  through (10). The ionic strength is sufficiently

$$(K_d)_0 = \alpha^2 f_{\pm}^2 C_0 / (1 - \alpha) \quad (10)$$

low,  $(3-7) \times 10^{-4} M$ , that the mean activity coefficient  $f_{\pm}$  may be calculated with sufficient accuracy from the Debye-Hückel limiting law, using the known values for the relative permittivity of acetonitrile<sup>20</sup> at each

(17) J. M. Smithson and R. J. P. Williams, *J. Chem. Soc.*, 457 (1958).

(18) T. E. Hogen-Esch and J. Smid, *J. Amer. Chem. Soc.*, **88**, 307, 318 (1966).

(19) This is in contrast to the value of  $80 M^{-1} \text{cm}^{-1}$  reported in ref 6. The reason for the large discrepancy is not clear.

(20) J. E. Timmermans, "Physico-Chemical Constants of Pure Organic Compounds," Vol. 2, Elsevier, Amsterdam, 1965, p 343.

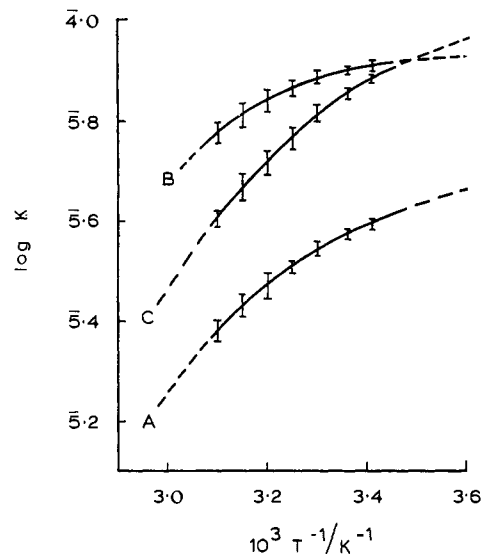


Figure 2. van't Hoff plots for equilibrium constants associated with (2); see text: A,  $\log (K_d)_0$ ; B,  $\log (K_s)_0$ ; C,  $\log (K_i)_0/(K_s)_0$ .

temperature. By combining (3), (7), (8), and (9) we obtain (11). The second term in the numerator is

$$K_i = \left( \frac{A}{\epsilon} - \alpha C_0 \right) / \left( C_0 - \frac{A}{\epsilon} \right) \quad (11)$$

10-25% of the first term, depending on the concentration, so that  $K_i$  is relatively insensitive to the value used for  $f_{\pm}$ . The values of  $K_i$  so derived were independent of ionic concentration and may therefore be regarded as identical with limiting values  $(K_i)_0$ , likewise for the  $K_s$  values derived from  $(K_d)_0$  and  $(K_i)_0$  through (6). It may be noted that at  $15^\circ$ ,  $K_i = 1$ ; i.e., the concentrations of  $\text{NiLCl}^+||\text{Cl}^-$  and  $\text{NiLCl}_2$  are equal.

The curved plot of  $\log (K_d)_0$  against  $T^{-1}$  may now be interpreted in terms of (6). At high temperatures (beyond the experimental range),  $K_i$  becomes small relative to 1 and the value of  $(K_d)_0$  tends to that of  $(K_i)_0(K_s)_0$ . At low temperatures (beyond the experimental range),  $K_i$  becomes large relative to 1 and the value of  $(K_d)_0$  tends to that of  $(K_s)_0$ . These relationships are shown in Figure 2 and the general behavior is similar to that found for sodium fluorenyl in tetrahydrofuran,<sup>18</sup> although in the present system we have been restricted to a much smaller temperature range. The curvature in the plots of  $\log (K_s)_0$  and  $\log (K_i)_0 \cdot (K_s)_0$  may be due to a change in the enthalpy values with temperature, but the experimental errors are such that it is not warranted to report other than the average values of  $\Delta H^\circ$  and  $\Delta S^\circ$  over the temperature range investigated; see Table I. (A plot of  $\log K_i$  against  $T^{-1}$  is linear and gives the values of  $\Delta H_i^\circ$  and  $\Delta S_i^\circ$  in Table I.) The enthalpy of ionization from  $\text{NiLCl}^+||\text{Cl}^-$  ( $\Delta H_s^\circ$ ) is less negative than the enthalpy of ionization from  $\text{NiLCl}_2$  ( $\Delta H_i^\circ + \Delta H_s^\circ$ ). For dissociation into ions from both species, the enthalpy of solvation outweighs the coulombic energy. The magnitude of  $\Delta S_i^\circ$  suggests<sup>21</sup> that only one additional solvent molecule is immobilized in going from  $\text{NiLCl}_2$  to  $\text{NiLCl}^+||\text{Cl}^-$  and this is presumably held weakly in a fifth coordinating position.

(21) J. Smid in "Ions and Ion Pairs in Organic Reactions," M. Szwarc, Ed., Wiley-Interscience, New York, N. Y., 1972, Chapter 3, p 109.

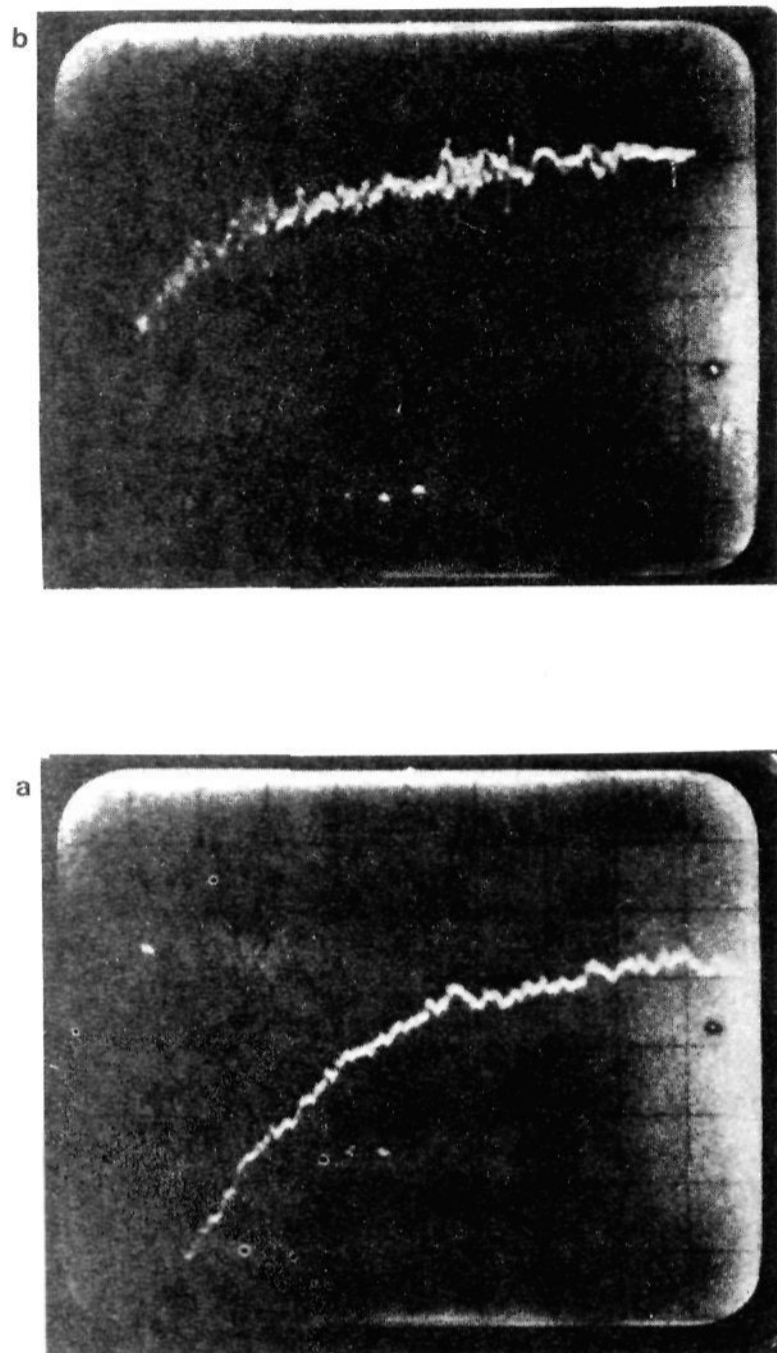


**Figure 3.** Relaxation traces: (a) laser pulse technique, absorbance change at 530 nm as a function of time in  $4 \times 10^{-3} M$  NiLCl<sub>2</sub> at 20°; vertical scale, 0.3% absorbance change/division (absorbance increasing downwards); horizontal scale, 0.5 μsec/division; laser pulse energy ~200 mJ; (b) DFE technique; vertical scale (0.5 V/division), change of voltage across the Wheatstone bridge on applying a field of 30 kV cm<sup>-1</sup> to the sample cell ( $C_0 = 1.61 \times 10^{-4} M$ ) and reference cell; horizontal scale, 1.0 μsec/division.

**Laser Experiments.** When a solution of NiLCl<sub>2</sub> in acetonitrile was irradiated at 1.06 μm with a Q-switched pulse from the laser, there was a rapid (0.5–7%) rise in the absorbance at 530 nm indicating an increased concentration of the species NiLCl<sup>+</sup>||Cl<sup>-</sup> and NiLCl<sup>+</sup>. The complex absorbs at the laser wavelength ( $\epsilon_{1060} \sim 10 M^{-1} \text{cm}^{-1}$ ), and we attribute the rise in absorbance to a photochemical displacement of (2). This point is considered in more detail elsewhere.<sup>22</sup> The net result is a rapid concentration jump in the system and the subsequent relaxation process may be analyzed to provide information on the kinetics of mechanism 2. The relaxation traces were exponential in form as shown in Figure 3(a), and the relaxation time  $\tau$  decreased with increasing concentration. At an overall concentration ( $C_0$ ) of  $10^{-2} \text{mol dm}^{-3}$ , the relaxation time approached a minimum value of 0.73 μsec at 20° (see Figure 4).

**Electric Field-Jump Experiments.** Figure 3(b) shows a relaxation trace obtained at 30 kV cm<sup>-1</sup>. The increase in molar conductance calculated from the asymptotic level in such traces was a linear function of field strength,

(22) J. J. McGarvey and J. Wilson, manuscript in preparation.

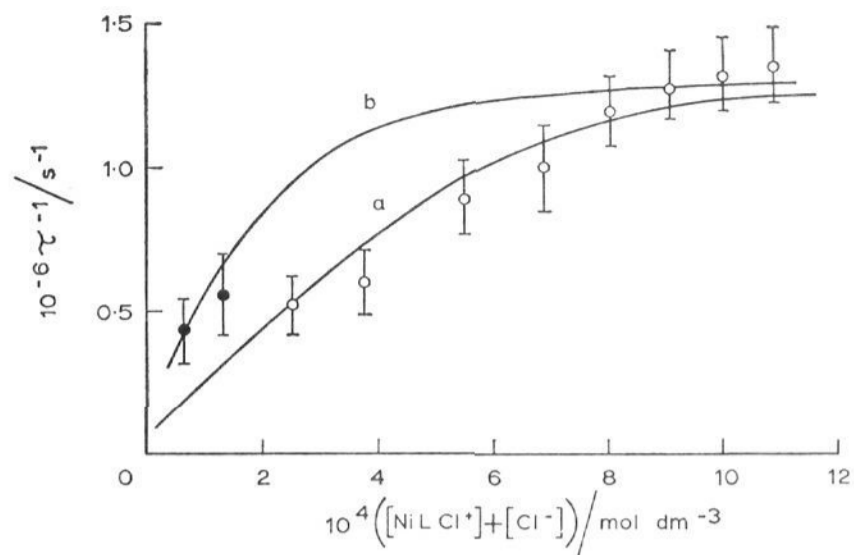


**Figure 4.** Dependence of reciprocal relaxation time  $\tau^{-1}$  on the concentration of free ions calculated from  $C_0$ ,  $(K_d)_0$ , and  $f_{\pm}$  by means of eq 10: O, laser experiments; ●, field-jump experiments. Temperature  $20 \pm 0.3^\circ$ . Lines a and b calculated from eq 14 with  $k_{32} = 2 \times 10^9$  and  $5 \times 10^9 M^{-1} \text{sec}^{-1}$ , respectively (see text).

**Table II.** Relaxation Times from Electric Field-Jump Studies on Solutions of NiLCl<sub>2</sub> in Acetonitrile (L = 1,1,7,7-tetraethyldiethylenetriamine)

Temp, °C	$10^5 C_0$ , mol dm <sup>-3</sup>	No. of relaxation traces	Av $\tau$ , μsec
20	16.1	4	1.8
	5.38	4	2.3
25	16.0	3	1.6
	5.34	4	2.0
30	15.9	2	1.5
	5.29	4	1.7
35	15.8	3	1.45
	5.24	4	1.6

as required by the Onsager theory<sup>23</sup> of the second Wien effect. This aspect of the work will be dealt with more fully elsewhere.<sup>24</sup>

As in the laser experiments, the relaxation traces were exponential in form and the (single) relaxation time decreased with increasing temperature and with increasing concentration (see Table II). For technical reasons the laser and DFE studies had to be conducted in concentration ranges which did not overlap. Nevertheless, as shown in Figure 4, the two sets of data are reasonably concordant. The experimental errors are such that one cannot be sure from the data whether the true relationship between  $\tau^{-1}$  and  $([\text{NiLCl}^+] + [\text{Cl}^-])$  is linear or curved. However, this can be partially resolved from a kinetic analysis and comparison with the thermodynamic data, as shown below.

**Treatment and Discussion of the Kinetic Results.** Since the thermodynamic results are in accord with mechanism 2, we use this scheme to interpret the relaxation measurements. Standard kinetic analysis<sup>25</sup> of (2) leads to the determinant

$$\begin{vmatrix} a_{11} - \frac{1}{\tau} & a_{12} \\ a_{21} & a_{22} - \frac{1}{\tau} \end{vmatrix} = 0 \quad (12)$$

(23) L. Onsager, *J. Chem. Phys.*, **2**, 599 (1934).

(24) H. Hirohara, K. J. Ivin, and J. J. McGarvey, *J. Amer. Chem. Soc.*, **96**, 3311 (1974).

(25) G. Czerninski, "Chemical Relaxation," Arnold, London, 1966, p 36; D. N. Hague, "Fast Reactions," Wiley, London, 1971, p 33.

in which the elements  $a_{ij}$  are defined by

$$a_{11} = k_{32}(\bar{c}_1 + \bar{c}_2 + K_s)$$

$$a_{12} = k_{32}K_s$$

$$a_{21} = k_{21}$$

$$a_{22} = k_{21}(1 + K_i)$$

where  $\bar{c}_1$  and  $\bar{c}_2$  denote the equilibrium concentrations of  $\text{NiLCl}^+$  and  $\text{Cl}^-$  calculated from (10). The two reciprocal relaxation times  $\tau_1^{-1}$  and  $\tau_2^{-1}$  characterizing the mechanism are the solutions of the quadratic equation (13), and are given respectively by the sum and difference

$$(\tau^{-1})^2 - (a_{11} + a_{22})(\tau^{-1}) + (a_{11}a_{22} - a_{12}a_{21}) = 0 \quad (13)$$

of the square-bracket terms in (14).

$$\tau_{1,2}^{-1} = \frac{1}{2}\{[a_{11} + a_{22}] \pm [(a_{11} + a_{22})^2 + 4(a_{12}a_{21} - a_{11}a_{22})]^{1/2}\} \quad (14)$$

In an attempt to identify the observed relaxation time with either the smaller  $\tau_1$  or the larger  $\tau_2$ , we now discuss the evaluation of the rate constants  $k_{21}$  and  $k_{32}$ . Consideration of the equilibrium constants and concentrations appearing in the expressions for  $a_{ij}$  shows that at high concentrations the term  $a_{12}a_{21}$  may be neglected in comparison with the term  $a_{11}a_{22}$ , and, from (14), the expressions for the reciprocal relaxation times are then given by (15) and (16)

$$\tau_1^{-1} = k_{32}(\bar{c}_1 + \bar{c}_2) + k_{23} \quad (15)$$

$$\tau_2^{-1} = k_{21}(1 + K_i) \quad (16)$$

According to (15), for a plot of  $\tau^{-1}$  against  $(\bar{c}_1 + \bar{c}_2)$  the ratio intercept/slope should be  $k_{23}/k_{32} = K_s$ . In fact, linear least-squares analysis of the data in Figure 4 yields a value of  $4 \times 10^{-4}$  for the ratio whereas (Table I)  $K_s = 8 \times 10^{-5}$ . The situation is somewhat worse for the linear relationship (17) to which (14) reduces when

$$\tau^{-1} = k_{32}(\bar{c}_1 + \bar{c}_2) + k_{23}K_i/(1 + K_i) \quad (17)$$

$a_{22} \gg a_{11}$ . In this case the ratio intercept/slope should be  $K_iK_s/(1 + K_i) = K_d = 3.9 \times 10^{-5}$ .

The experimental relaxation times become independent of concentration at high concentrations (Figure 4) suggesting that under these conditions the observed relaxation time approximates to  $\tau_2$ , given by (16). We may therefore use this solution to estimate  $k_{21}$ . Substituting the limiting value of  $\tau^{-1} = 1.37 \times 10^6 \text{ sec}^{-1}$  and  $K_i = 0.95$  (Table I) gives  $k_{21} = 7 \times 10^5 \text{ sec}^{-1}$  at  $20^\circ$ . This value of  $k_{21}$  may now be used to derive a preliminary value of  $k_{32}$  from the results at lower concentration, assuming that the observed relaxation times are solutions of (13). Rearranging (13) we obtain (18)

$$k_{32} = \frac{\tau^{-1}[k_{21}(1 + K_i) - \tau^{-1}]}{k_{21}(1 + K_i)(\bar{c}_1 + \bar{c}_2) + K_iK_s k_{21} - \tau^{-1}(\bar{c}_1 + \bar{c}_2 + K_s)} \quad (18)$$

Substitution of  $k_{21} = 7 \times 10^5 \text{ sec}^{-1}$ ,  $K_i$  and  $K_s$  from Table I, and the experimental  $\tau^{-1}$  values at  $20^\circ$  into (18) gave the range of values  $2\text{--}5 \times 10^9 \text{ M}^{-1} \text{ sec}^{-1}$  for  $k_{32}$ . Selected values of  $k_{32}$  in this range, together with  $k_{21}$ , were in turn substituted into (14) to obtain values for  $\tau_1$  and  $\tau_2$ . Those shown in Table III were obtained using  $k_{32} = 2.0 \times 10^9 \text{ M}^{-1} \text{ sec}^{-1}$ ; it may be

**Table III.** Comparison of Observed Relaxation Times at  $20^\circ$  with the Values Calculated from Eq 14 with  $k_{21} = 7 \times 10^5 \text{ sec}^{-1}$  and  $k_{32} = 2.0 \times 10^9 \text{ M}^{-1} \text{ sec}^{-1}$

$10^4(\bar{c}_1 + \bar{c}_2)$ , mol dm <sup>-3</sup>	$\tau_1$ , $\mu\text{sec}$	$\tau_2$ , $\mu\text{sec}$	$\tau(\text{obsd})$ , $\mu\text{sec}$
10.9	0.40	0.80	0.75
10.0	0.43	0.81	0.76
9.07	0.46	0.83	0.79
8.04	0.50	0.85	0.84
6.90	0.54	0.92	1.0
5.50	0.59	1.03	1.1
3.75	0.64	1.40	1.67
1.30	0.68	3.13	1.79
0.63	0.68	5.16	2.27

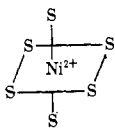
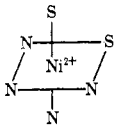
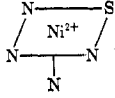
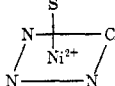
seen that there is reasonable agreement between the values of  $\tau_2$  and the observed  $\tau$  over most of the concentration range. The quantitative agreement is poor for the two lowest concentrations where in fact the observed  $\tau$  values are quite close to the average of the calculated  $\tau_1$  and  $\tau_2$ . The relaxation traces of conductivity changes recorded in the DFE experiments were rather noisy, and the precision of these results is lower than those derived from the optical density traces recorded in the laser pulse experiments. Work is now in progress in which the laser is coupled to a conductometric detection system. It is hoped that this more sensitive means of detection will allow measurements by the laser technique at low concentrations previously accessible only to the DFE method. It may therefore be possible to measure more precisely the relaxation times at low concentrations. The difficulty of exact experimental resolution of two relaxation times when they are not greatly different has been discussed by several authors.<sup>25,26</sup> Taking this into consideration here, the present values of  $k_{21} = 7 \times 10^5 \text{ sec}^{-1}$  and  $k_{32} = 2 \times 10^9 \text{ M}^{-1} \text{ sec}^{-1}$  are believed to be correct within 30%, the uncertainty in  $k_{21}$  being somewhat less than that in  $k_{32}$ . The calculated curve for these rate constants is shown in Figure 4 (lower curve). For comparison a second curve, calculated using a higher value for  $k_{32}$ , is also shown.

The kinetic data as well as the thermodynamic data can thus be satisfactorily accounted for in terms of (2). This scheme resembles that proposed to account for the behavior of alkali metal fluorenyls in ethereal solvents.<sup>18</sup> When written in reverse, it is also formally identical with the dissociative mechanism proposed by Eigen<sup>27</sup> to explain the kinetic behavior of aqueous complex formation reactions. The rate-determining step in such a mechanism is the dissociation of the metal-solvent bond. In the present case we assume that the species written  $\text{NiLCl}^+||\text{Cl}^-$  in fact has a solvent molecule weakly held in the fifth coordination position around the nickel atom so that  $k_{21}$  is identified with the splitting off of this weakly held solvent molecule. A comparison of  $k$  values for the breaking of  $\text{CH}_3\text{CN} \cdots \text{Ni}$  bonds in different species is shown in Table IV. It is seen that the ease of removal of the solvent molecule in  $[\text{NiLCl}(\text{CH}_3\text{CN})]^+$  is comparable with that in  $[\text{Ni}(\text{tren})(\text{CH}_3\text{CN})_2]^{2+}$  and much greater

(26) E.g., E. J. del Rosario and G. G. Hammes, *J. Amer. Chem. Soc.*, **92**, 1750 (1970).

(27) M. Eigen in "Advances in the Chemistry of the Coordination Compounds," S. Kirschner, Ed., Macmillan, New York, N. Y., 1961, p 373.

**Table IV.** Rate Constants for the Breaking of  $\text{CH}_3\text{CN} \cdots \text{Ni}$  Bonds in Various Species at the Temperatures Indicated ( $^\circ\text{C}$ )

Reacting species <sup>a</sup>	Notional geometry <sup>b</sup>	$10^{-3}k$ , $\text{sec}^{-1}$
$[\text{Ni}(\text{CH}_3\text{CN})_6]^{2+}$		$0.34^c, d$ ( $25^\circ$ )
$[\text{Ni}(\text{tren})(\text{CH}_3\text{CN})_2]^{2+}$		$165^d, e$ ( $25^\circ$ ) $\geq 2000^d, f$ ( $-40^\circ$ )
$[\text{Ni}(\text{Me}_6\text{tren})(\text{CH}_3\text{CN})]^{2+}$		$<0.1^d$ ( $80^\circ$ )
$[\text{NiLCl}(\text{CH}_3\text{CN})]^+$		$700^g$ ( $20^\circ$ )

<sup>a</sup> tren =  $(\text{H}_2\text{NCH}_2\text{CH}_2)_3\text{N}$ ; Me<sub>6</sub>tren =  $(\text{Me}_2\text{NCH}_2\text{CH}_2)_3\text{N}$ ; L =  $(\text{Et}_2\text{NCH}_2\text{CH}_2)_2\text{NH}$ . <sup>b</sup> The actual geometries may be distorted forms of the structures indicated; S = solvent  $\text{CH}_3\text{CN}$ . <sup>c</sup> Corrected for a statistical factor of 6. <sup>d</sup> R. J. West and S. F. Lincoln, *Inorg. Chem.*, **12**, 494 (1973). <sup>e</sup> S trans to tertiary N of tren. <sup>f</sup> S cis to tertiary N of tren. <sup>g</sup> This work.

than in  $[\text{Ni}(\text{CH}_3\text{CN})_6]^{2+}$ . In this as in other systems<sup>28</sup> a strongly held ligand weakens the bonds to the remaining solvent molecules. It should be borne in mind

(28) W. J. McKellar and D. B. Rorabacher, *J. Amer. Chem. Soc.*, **93**, 4379 (1971).

that the above discussion is based on the assumption of the dissociative exchange mechanism of Eigen.<sup>27</sup> There is some evidence that this does not always apply in nonaqueous solvents<sup>29</sup> and one cannot rule out the possibility of a second-order solvent- or ligand-assisted exchange in some cases.

Turning now to the value of  $k_{32}$  we may note that it approaches the value expected for a diffusion-controlled reaction. In line with this, preliminary investigations using the laser technique show that the activation energy is of the same order of magnitude as the quantity  $B$  defined by the expression for the temperature variation of solvent viscosity,  $\eta \propto \exp(B/RT)$ .

### Conclusions

The thermodynamic results strongly support the mechanism denoted by (2) involving the participation of the species  $\text{NiLCl}^+ \cdots \text{Cl}^-$  in which the solvent  $\text{CH}_3\text{CN}$  is weakly bound in the fifth coordination position. The mechanism also allows a satisfactory interpretation of the kinetic data and it appears that under the experimental conditions employed the interconversion of  $\text{NiLCl}^+ \cdots \text{Cl}^-$  and five-coordinate  $\text{NiLCl}_2$  is not rate determining in the readjustment of the successive equilibria following perturbation.

**Acknowledgments.** We thank the Queen's University of Belfast for the award of a postdoctoral fellowship to H. H. One of us (H. H.) acknowledges helpful discussions with Professors R. G. Pearson and M. L. Bender. We are grateful to the Science Research Council for a grant in support of this research.

(29) E. F. Caldin and M. W. Grant, *J. Chem. Soc., Faraday Trans. 1*, **69**, 1648 (1973).

## Stereochemistry of Cobalt Porphyrins. I. The Structure and Characterization of 2,3,7,8,12,13,17,18-Octaethylporphinato-bis(3-methylpyridine)cobalt(II)

Robert G. Little and James A. Ibers\*

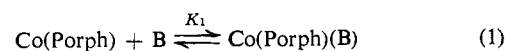
Contribution from the Department of Chemistry, Northwestern University, Evanston, Illinois 60201. Received December 28, 1973

**Abstract:** The six-coordinate Co(II) porphyrin,  $\text{Co}(\text{3-pic})_2(\text{OEP})$  (3-pic = 3-picoline = 3-methylpyridine), has been prepared and characterized by a complete X-ray structural determination. The structure has been refined anisotropically to a final conventional  $R$  value (on  $F$ ) of 0.036 based on 3628 values of  $F_o^2$  above background. The complex crystallizes in the triclinic space group  $C_1^1-P\bar{1}$  with  $a = 10.187$  (3) Å,  $b = 11.258$  (4) Å,  $c = 9.753$  (3) Å,  $\alpha = 93.10$  (2)°,  $\beta = 92.32$  (2)°,  $\gamma = 113.28$  (2)°, and  $Z = 1$ . Hence the molecule has a crystallographically imposed center of symmetry. The axial Co-N(3-pic) bond length of 2.386 (2) Å is long compared with the average equatorial Co-N bond length of 1.992 (1) Å. The lengthening of the axial bond is attributed to the occupancy of the  $d_{z^2}$  orbital by a single unpaired electron.

**S**olution studies of Co(II) porphyrins<sup>1-5</sup> have shown that these complexes add one or two molecules of

- (1) F. A. Walker, *J. Amer. Chem. Soc.*, **92**, 4235 (1970).
- (2) D. V. Stynes, H. C. Stynes, B. R. James, and J. A. Ibers, *J. Amer. Chem. Soc.*, **95**, 1790 (1973).
- (3) F. A. Walker, *J. Amer. Chem. Soc.*, **95**, 1150 (1973).
- (4) F. A. Walker, *J. Amer. Chem. Soc.*, **95**, 1154 (1973).
- (5) B. M. Hoffman and D. H. Petering, *Proc. Nat. Acad. Sci. U. S.*, **67**, 637 (1970).

various nitrogenous bases to form five- and six-coordinate complexes.



The equilibria and thermodynamics of these reactions have been studied in some detail by esr<sup>3</sup> and visible